NASA TECHNICAL NOTE

NASA TN D-2209

NASA TN D-2209

FLOW AND HEAT TRANSFER BETWEEN HEATED PLATES OF FINITE LENGTH IN A FREE-MOLECULE FLOW ENVIRONMENT

by Morris Perlmutter

Lewis Research Center

Cleveland, Ohio

NATIONAL AERONAUTICS AND SPACE ADMINISTRATION • WASHINGTON, D. C. • OCTOBER 1964

FLOW AND HEAT TRANSFER BETWEEN HEATED PLATES OF FINITE LENGTH IN A FREE-MOLECULE FLOW ENVIRONMENT

By Morris Perlmutter

Lewis Research Center
Cleveland, Ohio

NATIONAL AERONAUTICS AND SPACE ADMINISTRATION

For sale by the Office of Technical Services, Department of Commerce,
Washington, D.C. 20230 -- Price $1.00

FLOW AND HEAT TRANSFER BETWEEN HEATED PLATES OF FINITE LENGTH IN A FREE-MOLECULE FLOW ENVIRONMENT

by Morris Perlmutter

Lewis Research Center

SUMMARY

Solutions for the mass-flow profiles, density, static pressure, temperature, and wall shear distributions for a collisionless gas flowing through a finite length flat-plate channel are given, and numerical values for particular cases are calculated. The heat transfer between the channel walls and the environment are calculated for the rarefied gas heat transfer as well as for radiant heat transfer. The results indicate that the rarefied gas heat transfer can be significant compared with the thermal radiation for conditions similar to those that occur in a thermionic converter.

INTRODUCTION

There is a growing interest in rarefied gas flow and heat transfer because of the low-density environment that is being encountered in present-day technology. When the mean free path of the molecules is small compared with the model dimensions, the fluid may be treated macroscopically and the classical Navier-Stokes equations used. When the mean free path of the molecule is large, however, these limiting equations no longer apply. These cases can be treated by using the kinetic theory of gases. The limiting case treated by kinetic theory, namely, that of very large mean free paths, which is called free-molecule flow, is considered herein.

The problem of free-molecule-flow heat transfer between infinite plates was treated by Knudsen, as discussed in reference 1. The problem of heat transfer in an adiabatic tube and nozzle with free-molecule flow was treated in references 2 and 3. The heat transfer to a nonconvex surface from a free-molecule stream was treated in reference 4.

The model analyzed here consists of a flat-plate channel of finite length and infinite depth with each plate isothermal at a different uniform temperature. The accommodation coefficients for both plates are assumed uniform and equal. There are assumed to be no intermolecular collisions in the channel. The channel connects two gas reservoirs, each reservoir fixed at a given temperature and density. The mass transfer flow rate through the channel formed by the plates is found by numerically integrating the exact integral equation.

The longitudinal and transverse flow distributions as well as the density and wall shear distributions in the channel are given. (From these distributions, the local pressure and temperature can be calculated.) The total energy leaving the surface is calculated, and the net energy transferred between the surfaces and the environment is found. In addition, the thermal radiation heat transfer is calculated for a similar model, and the heat transferred by radiation is compared with that for free-molecule flow for a situation that might be applicable to the analysis of heat transfer in thermionic energy converters.

SYMBOLS

A_L, A_R	cross-sectional areas of inlet and outlet, respectively
A_λ, A_μ	areas of lower and upper plate, respectively
c_v	heat capacity at constant volume
E	energy per unit mass of molecular stream, $[c_v + (R/2)]T$
e	energy flux leaving surface
$e_{\lambda_1,t}$	total energy flux (emitted and reflected) leaving surface λ at location λ_1
F	shape factor
f	mass-flow ratio, $(m - m_R)/(m_L - m_R)$
f_V	number of molecules per unit volume having velocity V per unit velocity interval
K	kernel, (see eq. (3))
L_m	mean free path
l	length of plates divided by distance between them
M	mass of molecule
$\mathcal{M}$	molecular weight
m	mass-flow rate per unit area (mass flux)
m_L	mass flux entering the channel from left reservoir, $\rho_L/2\pi^{1/2}\beta_L$
m_{L-R}	average mass flux through channel from left to right reservoir
p_s	static pressure
Q	total rate of heat loss from surface

R	gas constant, $\frac{1.987}{\mathcal{M}} \frac{\text{cal}}{(^{\circ}\text{K})(\text{g})}$
r	distance shown in fig. 1 (p. 5)
s	distance shown in fig. 1 (p. 5)
T	temperature
T_s	static temperature
U	average nontranslational internal energy of the molecule
u	mean velocity
u_1,u_2	component of mean velocity in x_1- and x_2-directions, respectively
V	velocity of molecule
V'	undirected component of velocity
x_1,x_2,x_3	space coordinates divided by distance between plates (see fig. 1(a), p. 5)
x'	a position location
α	accommodation coefficient (emissivity)
β	$1/(2RT)^{1/2}$
θ	angle shown in fig. 1 (p. 5) measured clockwise from normal to surface
θ_0,θ_l	angles beginning of plate and to end of plate, respectively (see fig. 1(a), p. 5)
λ_1,λ_3	coordinates on lower plate divided by distance between plates in x_1- and x_3-directions, respectively
μ_1,μ_3	coordinates on upper plate divided by distance between plates in x_1- and x_3-directions, respectively
ρ	density
ρ_s	density at standard conditions (273° K and 1 atm)
σ	Stefan-Boltzmann constant, 1.36×10^{-12} cal/(sec)(cm^2)($^{\circ}$K^4)
σ_m	molecular diameter
τ_{x_1,x_2}	shear stress

φ subsolutions as given by eqs. (30) to (34)

$\overline{\varphi}$ $\frac{1}{l}\int_0^l \varphi \, dx$

$\overline{\varphi F}$ $\frac{1}{l}\int_0^l \varphi F \, dx$

ψ angle from normal to element

Subscripts:

A-B from point A to point B

a contribution from environment above x_2

b contribution from environment below x_2

c convected heat transfer

i isothermal case, walls and reservoirs at same temperature

in incident

L left environment

l to right end of channel

o to left end of channel

R right environment

r radiated heat transfer

t total leaving surface including reflected and emitted streams

w on wall surface

θ in direction θ

λ lower wall

μ upper wall

Superscripts:

$(\bar{\ })$ mean, $\int_0^\infty (\ )f_v \, dV$

$(\hat{\ })_1,(\hat{\ })_2$ $l - (\ )_1,\ 1 - (\ )_2$

ANALYSIS

The model analyzed consists of two parallel plates whose length divided by the distance between them is l. The plates are of infinite depth and are at temperatures T_λ and T_μ, respectively. The left and right environments are at temperatures T_L and T_R and densities ρ_L and ρ_R, respectively, as shown in figure 1(a). The gas is in equilibrium in the left and right reservoirs. The density of the gas is assumed to be sufficiently low everywhere so that the mean free path of the molecules is large with respect to the distance between the plates. In this model, therefore, the effect of intermolecular collisions in the channel is small and may be neglected.

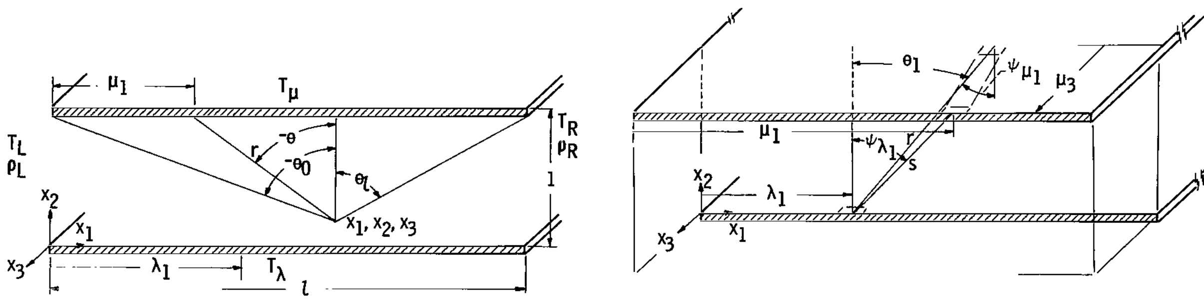

(a) Space element. (b) Wall element.

Figure 1. - Analytical model.

Mass Flux Leaving Walls

The total mass flux leaving the lower plate at a point having an x_1-coordinate equal to λ_1 is denoted by m_{λ_1}. This is equal to the mass flux incident at that point. The flux incident (and leaving) the lower wall as derived in the appendix (eq. (A5)) is given by

$$m_{\lambda_1} = \frac{1}{2} \int_{\theta=-\pi/2}^{\pi/2} m_\theta \; d(\sin \theta) \tag{1}$$

where m_θ is the mass flux emitted from the surface element that is oriented at angle θ with respect to the normal from the point λ_1 on the lower plate as shown in figure 1(b). For the present case, this becomes

$$m_{\lambda_1} = \frac{m_L}{2} \int_{-\pi/2}^{\theta_0} d(\sin \theta) + \int_{\theta_0}^{\theta_l} \frac{m_\theta}{2} \, d(\sin \theta) + \frac{m_R}{2} \int_{\theta_l}^{\pi/2} d(\sin \theta) \tag{2}$$

where m_L and m_R are the mass fluxes entering the channel from the left and right environments. If m_θ and m_L are equal to m_R, then equation (2) shows that m_{λ_1} equals m_R. Hence, equation (2) may be written as

$$f_{\lambda_1} = \frac{m_{\lambda_1} - m_R}{m_L - m_R} = \int_{-\pi/2}^{\theta_0} \frac{d(\sin\theta)}{2} + \int_{\theta_0}^{\theta_l} f_\theta \frac{d(\sin\theta)}{2} \tag{3a}$$

or

$$f_{\lambda_1} = F_{dA_{\lambda_1}-L} + \int_{\mu_1=0}^{l} f_{\mu_1} K(\lambda_1,\mu_1) d\mu_1 \tag{3b}$$

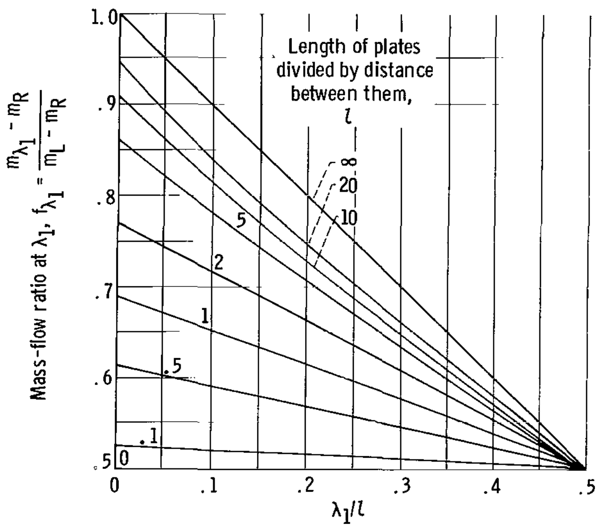

Figure 2. - Mass-flow ratio from surface.

where $F_{dA_{\lambda_1}}$ and $K(\lambda_1,\mu_1)d\mu_1$ are given in the appendix by equations (A7) and (A8). The solution to equation (3b) was obtained by numerical integration and iteration. The results are shown in figure 2 for various values of l, and table I gives numerical values of f for $\lambda_1 = 0$. From the symmetry of the problem, f_{μ_1} along the upper plate has the same functional dependence on μ_1 as f_{λ_1} has on λ_1 or $f_{\mu_1} = f_{\lambda_1}\Big|_{\lambda_1=\mu_1}$. The function f_{λ_1} satisfies the relation of $f_{\lambda_1} + f_{\hat{\lambda}_1} = 1$, where $\hat{\lambda}_1 = l - \lambda_1$. This relation is discussed in reference 2 and agrees with the numerical results reported herein.

TABLE I. - VALUES OF MASS-FLOW RATIO AT ENTRANCE OF CHANNEL

Length of plates divided by distance between them, l	Mass-flow ratio at entrance of channel, f_0
0.1	0.5249
.5	.6132
1	.6883
2	.7701
5	.8627
10	.9141
20	.9485
∞	1.0

Average Longitudinal Mass Flux

The average mass flux through the channel can be found from

$$m_{L-R} = m_L - 2\int_0^l m_{\lambda_1} F_{dA_{\lambda_1}-L}\, d\lambda_1 - \left(m_R - 2\int_0^l m_R F_{dA_{\lambda_1}-R}\, d\lambda_1\right) \tag{4}$$

The first term on the right is the mass flux entering the channel at $x_1 = 0$; the second term is the mass flux leaving through the entrance ($x_1 = 0$) that comes from both the upper and lower walls. The factor 2 that appears in the second term takes account of the fact that, by symmetry, the mass flux leaving the upper wall that goes through the inlet is equal to the amount leaving the lower wall. The remaining terms give the mass flux leaving the inlet that enters the right end and has no collision with the wall. Since it can be shown that

$$\int_0^l F_{dA_{\lambda_1}-L}\, d\lambda_1 = \int_0^l F_{dA_{\lambda_1}-R}\, d\lambda_1$$

equation (4) can be rewritten as

$$\frac{m_{L-R}}{m_L - m_R} = 1 - 2\int_0^l f_\lambda F_{dA_{\lambda_1}-L}\, d\lambda_1 \qquad (5)$$

The average mass flux through the channel is shown in figure 3. It can be seen that

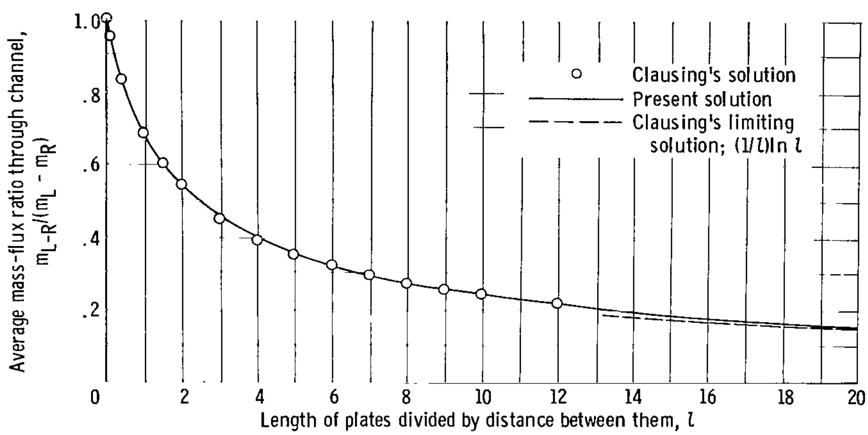

Figure 3. - Average mass flux through channel.

the average mass flux decreases for increasing lengths. Also shown in figure 3 is the approximate solution of Clausing (ref. 5), which was obtained by assuming a linear form of f_{λ_1} with an added correction factor. It can be seen that Clausing's approximate solution is in good agreement with the exact solution obtained by use of equation (5).

Density Distribution in Channel

As shown in the appendix, the density at a point (x_1,x_2) is given by equation (A11)

$$\rho = \int_0^{2\pi} \frac{\beta_\theta m_\theta}{\pi^{1/2}}\, d\theta \tag{6}$$

where the angle θ is again measured clockwise with respect to the normal to the upper plate passing through the point (x_1,x_2).

The total contribution to ρ at (x_1,x_2) from that part of the environment above x_2 is

$$\rho_a = \frac{\beta_L m_L}{\pi^{1/2}} \int_{-\pi/2}^{\theta_0} d\theta + \frac{\beta_R m_R}{\pi^{1/2}} \int_{\theta_l}^{\pi/2} d\theta + \frac{1}{\pi^{1/2}} \int_{\theta_0}^{\theta_l} \beta_\theta m_\theta\, d\theta \tag{7}$$

The first two terms are the contributions to the densities from the right and left reservoirs, and the remainder is the contribution from the upper wall. If $\beta_L m_L = \beta_R m_R = \beta_\theta m_\theta$, this equation reduces to the relation $\rho_a = \beta_R m_R 2\pi^{1/2}/2 = \rho_R/2$. For the isothermal case, where the walls and reservoirs are all at the same temperature, equation (7) may be written as

$$2\pi\left(\frac{\rho_a - \frac{\rho_R}{2}}{\rho_L - \rho_R}\right)_i = \int_{-\pi/2}^{\theta_0} d\theta + \int_{\theta_0}^{\theta_2} f_\theta\, d\theta \tag{8a}$$

since $\beta_L = \beta_R = \beta_\theta$. This can be readily generalized to the nonisothermal case.

By symmetry the contribution from the environment below x_2 is given by the same relation except that x_2 is replaced by $1 - x_2 \equiv \hat{x}_2$; that is,

$$\rho_{b,i}(x_1,x_2) = \rho_{b,i}(x_1,x_2)\Big|_{x_2=\hat{x}_2} \tag{8b}$$

so that the total density is

$$\left(\frac{\rho - \rho_R}{\rho_L - \rho_R}\right)_i = \left(\frac{\rho_b - \frac{\rho_R}{2}}{\rho_L - \rho_R}\right)_i + \left(\frac{\rho_b - \frac{\rho_R}{2}}{\rho_L - \rho_R}\right)_i \tag{8c}$$

If the reservoirs were reversed, then, in general, the density at the point $(\hat{x}_1,x_2)$ under reversed conditions would be equal to the density at (x_1,x_2) before reversal or

$$\left[\frac{\rho(\hat{x}_1,x_2) - \rho_L}{\rho_R - \rho_L}\right]_i = \left[\frac{\rho(x_1,x_2) - \rho_R}{\rho_L - \rho_R}\right]_i$$

which can be rewritten as follows:

$$\left[\frac{\rho(x_1,x_2) - \rho_R}{\rho_L - \rho_R}\right]_i + \left[\frac{\rho(\hat{x}_1,x_2) - \rho_R}{\rho_L - \rho_R}\right]_i = 1 \tag{9}$$

Thus the density values in the exit half of the channel may be found from the density values in the entrance half.

A reasonable approximation for f, as can be seen from figure 2 (p. 6), is a linear function of the x_1-coordinate, in particular,

$$f_\theta = f_0 + \frac{1 - 2f_0}{l}\mu_1 = f_0 + \frac{1 - 2f_0}{l}x_1 + \frac{1 - 2f_0}{l}\hat{x}_2 \tan\theta \tag{10}$$

Substituting equation (10) into equation (8a) and employing equations (8b) and (8c) give the following approximate result for the density:

$$\begin{aligned}
2\pi\left(\frac{\rho - \rho_R}{\rho_L - \rho_R}\right)_i &= \tan^{-1}\frac{\hat{x}_2}{x_1} + \tan^{-1}\frac{x_2}{x_1} \\
&+ \left(f_0 + \frac{1 - 2f_0}{l}x_1\right)\left(\tan^{-1}\frac{\hat{x}_1}{\hat{x}_2} + \tan^{-1}\frac{\hat{x}_1}{x_2} + \tan^{-1}\frac{x_1}{\hat{x}_2} + \tan^{-1}\frac{x_1}{x_2}\right) \\
&+ \frac{1 - 2f_0}{2l}\left[\hat{x}_2 \ln\left(\frac{\hat{x}_1^2 + x_2^2}{x_1^2 + \hat{x}_2^2}\right) + x_2 \ln\left(\frac{\hat{x}_1^2 + x_2^2}{x_1^2 + x_2^2}\right)\right]
\end{aligned} \tag{11}$$

These results are plotted in figure 4 for values of x_1 from 0 to $l/2$. (The remaining values can be found from eq. (9).) The values of f_0 are given in table I (p. 6).

Local Longitudinal Mass Flux

As shown in the appendix (eq. (A13)), the local mass flux through the channel at point (x_1,x_2) is given by

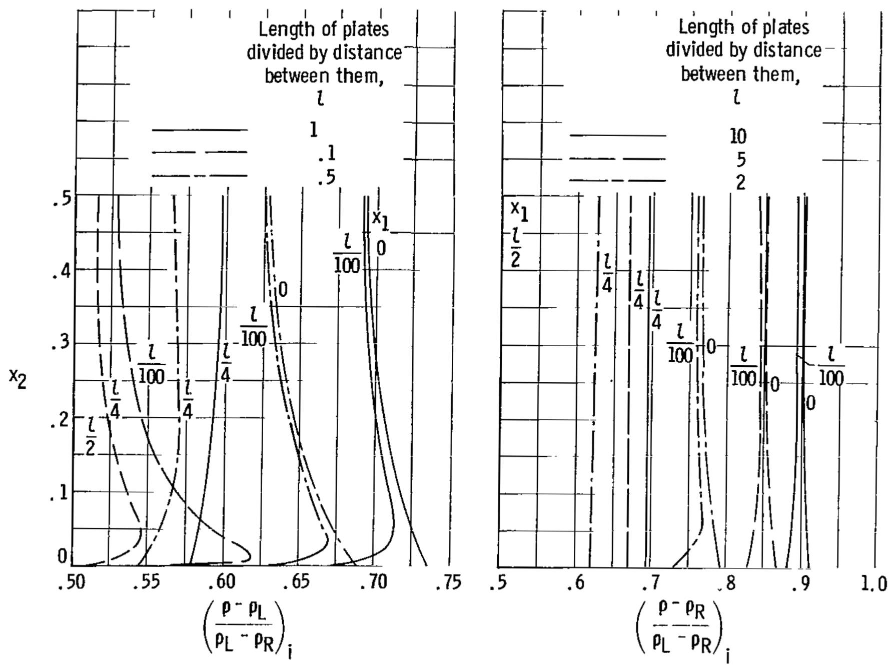

(a) Length of plates divided by distance between them, 1, 0.5, and 0.1.

(b) Length of plates divided by distance between them, 2, 5, and 10.

Figure 4. - Isothermal density distribution.

$$\rho u_1 = -\int_0^{2\pi} \frac{m_\theta}{2} \sin \theta \, d\theta \tag{12}$$

The contribution to ρu_1 at (x_1,x_2) arising from the environment above x_2 is

$$2(\rho u_1)_a = -m_L \int_{-\pi/2}^{\theta_0} \sin \theta \, d\theta - m_R \int_{\theta_l}^{\pi/2} \sin \theta \, d\theta - \int_{\theta_0}^{\theta_l} m_\theta \sin \theta \, d\theta \tag{13}$$

If $m_L = m_R = m_\theta$, then $(\rho u_1)_a = 0$ and equation (13) can be simplified to

$$\frac{2(\rho u_1)_a}{m_R - m_L} = \int_{-\pi/2}^{\theta_0} \sin \theta \, d\theta + \int_{\theta_0}^{\theta_l} f_\theta \sin \theta \, d\theta \tag{14}$$

The contribution to ρu_1 at (x_1,x_2) arising from the environment below x_2 is given by equation (14) evaluated at $\hat{x}_2$ instead of x_2, that is, $(\rho u_1)_b(x_1,x_2) = (\rho u_1)_a(x_1,x_2)\Big|_{x_2=\hat{x}_2}$, and the total longitudinal mass flow is given by $\rho u_1 = (\rho u_1)_a + (\rho u_1)_b$. Assuming the linear form of f given by equation (10) and integrating give

$$\frac{\rho u_1}{m_L - m_R} = \frac{1 - f_0}{2}\left[\frac{\hat{x}_2}{\left(\hat{x}_2^2 + x_1^2\right)^{1/2}} + \frac{\hat{x}_2}{\left(\hat{x}_2^2 + \hat{x}_1^2\right)^{1/2}}\right.$$

$$\left. + \frac{x_2}{\left(x_2^2 + x_1^2\right)^{1/2}} + \frac{x_2}{\left(x_2^2 + \hat{x}_1^2\right)^{1/2}}\right] + \frac{1 - 2f_0}{2l}$$

$$\times\left\{\hat{x}_2 \ln\left[\frac{\left(\hat{x}_1^2 + \hat{x}_2^2\right)^{1/2} - \hat{x}_1}{\left(x_1^2 + \hat{x}_2^2\right)^{1/2} + x_1}\right] + x_2 \ln \frac{\left(\hat{x}_1^2 + x_2^2\right)^{1/2} - \hat{x}_1}{\left(x_1^2 + x_2^2\right)^{1/2} + x_1}\right\} \tag{15a}$$

These results are plotted in figure 5.

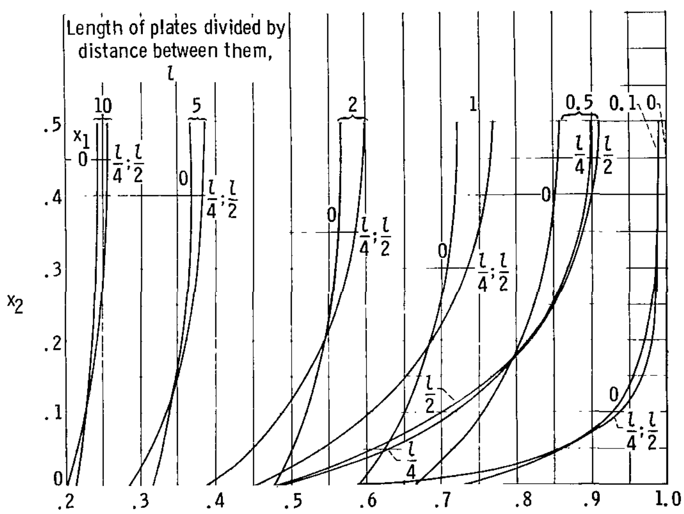

Figure 5. - Axial mass-flow profile.

Note from equation (15a) that the curves are symmetric about $x_1 = l/2$; that is,

$$\left(\frac{\rho u_1}{m_L - m_R}\right)_{x_1} = \left(\frac{\rho u_1}{m_L - m_R}\right)_{\hat{x}_1} \tag{15b}$$

This can be seen from the fact that the problem is symmetrical, so that, if the exit and entrance reservoirs are reversed, the result is

$$\left(\frac{\rho u_1}{m_R - m_L}\right)_{x_1} = -\left(\frac{\rho u_1}{m_L - m_R}\right)_{\hat{x}_1}$$

which is equal to equation (15b). The curves become less flat as the center of the channel is approached. The curves are symmetric around $x_1 = l/2$ and $x_2 = 0.5$.

Local mass flux in transverse or x_2-direction. - As shown in the appendix (eq. (A16)), the flux in the transverse direction is

$$\rho u \;=\; -\int_0^{2\pi} \frac{m_\theta}{2} \cos\,\theta\; d\theta \tag{16}$$

The contribution from the environment above x_2 is given by

$$2(\rho u_2)_a = -m_L \int_{-\pi/2}^{\theta_0} \cos\,\theta\; d\theta - m_R \int_{\theta_l}^{\pi/2} \cos\,\theta\; d\theta - \int_{\theta_0}^{\theta_l} m_\theta \cos\,\theta\; d\theta \tag{17}$$

If $m_\theta = m_L = m_R$, then $(\rho u_2)_a = -m_R$ and equation (17) reduces to

$$\frac{2(\rho u_2)_a + 2m_R}{m_R - m_L} = \int_{-\pi/2}^{\theta_0} \cos\,\theta\; d\theta + \int_{\theta_0}^{\theta_l} f_\theta \cos\,\theta\; d\theta \tag{18}$$

The contribution to the transverse flow from the lower wall is by symmetry the same as from the upper wall with x_2 replaced by $1 - x_2$ and with the sign changed:

$$(\rho u_2)_{b,x_2} = -(\rho u_2)_{a,\hat{x}_2}$$

Assuming the linear form for f (eq. (10)) and integrating give

$$\frac{2\rho u_2}{m_L - m_R} = (1 - f_0)\left[\frac{x_1}{\left(x_1^2 + \hat{x}_2^2\right)^{1/2}} - \frac{\hat{x}_1}{\left(\hat{x}_1^2 + \hat{x}_2^2\right)^{1/2}} + \frac{\hat{x}_1}{\left(x_2^2 + \hat{x}_1^2\right)^{1/2}} - \frac{x_1}{\left(x_2^2 + x_1^2\right)^{1/2}}\right]$$

$$- \frac{1 - 2f_0}{l}\left[\left(\hat{x}_2^2 + x_1^2\right)^{1/2} - \left(\hat{x}_2^2 + \hat{x}_1^2\right)^{1/2} - \left(x_2^2 + x_1^2\right)^{1/2} + \left(x_2^2 + \hat{x}_1^2\right)^{1/2}\right] \tag{19}$$

Notice that $(\rho u_2)_{x_2} = -(\rho u_2)_{\hat{x}_2}$ and also that $(\rho u_2)_{x_1} = -(\rho u_2)_{\hat{x}_1}$. Some of these results are shown in figure 6.

Shear stress along wall. - The shear stress on the lower wall in the x_1-direction is given by $\tau_{x_1,x_2} = -(\rho V_1' V_2')_w$, where V_1' is the local undirected component of molecule speed in the x_1-direction (i.e., $V_1' = V_1 - u_1$, where $\int_0^\infty V_1' f_V\; dV = 0$) and V_2' is the local undirected component of molecule speed in the x_2-direction (i.e., $V_2' = V_2 - u_2$, where $\int_0^\infty V_2' f_V\; dV = 0$).

Since the u_2 velocity is zero at the wall, the wall shear stress τ_{x_1,x_2}

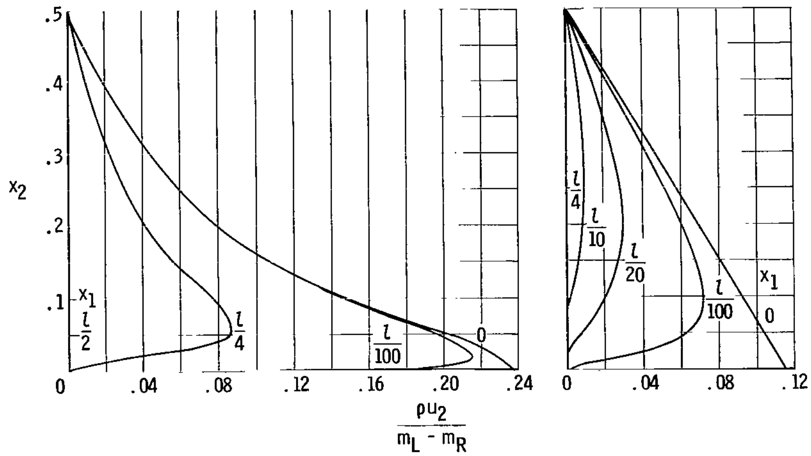

(a) Length of plates divided by distance between them, 0.1.

(b) Length of plates divided by distance between them, 2.

Figure 6. - Radial mass-flow profile.

can be written $-(\rho\overline{V_1V_2})_w$. Then by equation (A19),

$$(\rho\overline{V_1V_2})_w = \int_{\theta=-\pi/2}^{+\pi/2} \frac{m_\theta}{\beta_\theta \pi^{1/2}} \cos\theta \sin\theta \, d\theta \tag{20}$$

The contribution to the shear stress due to the molecules leaving the wall is zero since they are reflected diffusely. For the isothermal case, this becomes

$$\left(\frac{\beta\pi^{1/2}\rho\overline{V_1V_2}}{m_L - m_R}\right)_{w,i} = \int_{-\pi/2}^{\theta_0} \cos\theta \sin\theta \, d\theta + \int_{\theta_0}^{\theta_l} f_\theta \cos\theta \sin\theta \, d\theta \tag{21}$$

which can be integrated to give

$$\left(\frac{\rho\overline{V_1V_2}}{\frac{m_L^2}{\rho_L} - \frac{m_R^2}{\rho_R}}\right)_{w,i} = -\frac{1}{\lambda_1^2 + 1} + \left(f_0 + \frac{1 - 2f_0}{l}\lambda_1\right)\left(\frac{\hat{\lambda}_1^2}{\hat{\lambda}_1^2 + 1} - \frac{\lambda_1^2}{\lambda_1^2 + 1}\right)$$

$$+\left(\frac{1 - 2f_0}{l}\right)\left(\tan^{-1}\hat{\lambda}_1 + \tan^{-1}\lambda_1 - \frac{\hat{\lambda}_1}{\hat{\lambda}_1^2 + 1} - \frac{\lambda_1}{\lambda_1^2 + 1}\right) \tag{22}$$

The results are shown in figure 7.

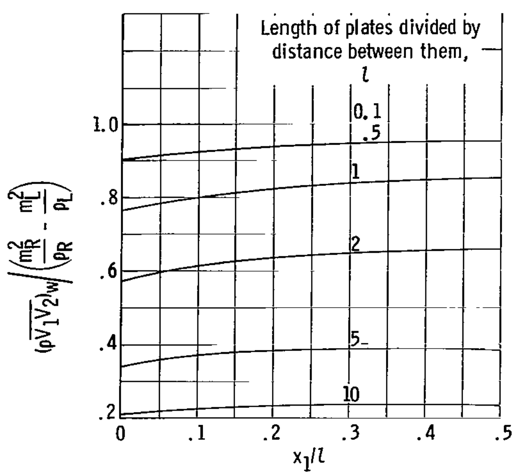

Figure 7. - Wall shear distribution.

<u>Local temperature and pressure in channel.</u> - The kinetic energy of the gas at a particular location due to an element $d\mu_1\ d\mu_3$ is given by

$$\int_{V=0}^{\infty} \frac{1}{2} V^2\ d\rho_{d\mu_1 d\mu_3, dV}$$

Following the same procedure used before results in

$$\frac{\rho\overline{V^2}}{2} = \frac{3}{4\pi^{1/2}} \int_0^{2\pi} \frac{m_\theta}{\beta_\theta}\ d\theta \tag{23}$$

The average kinetic energy of the gas can be expressed in terms of the local static temperature by writing

$$\frac{\rho\overline{V^2}}{2} = \frac{\rho\overline{(V' + u)^2}}{2} = \frac{\rho\overline{V'^2}}{2} + \frac{\rho u^2}{2} = \frac{3}{2}\ \rho R T_s + \frac{\rho u^2}{2} \tag{24}$$

where the kinetic theory definition has been used for the local static temperature T_s.

For the isothermal case, where walls and reservoirs are at temperature T, equation (6) becomes

$$\int_0^{2\pi} m_\theta\ d\theta = \frac{\rho(\pi)^{1/2}}{\beta}$$

Substituting this into equations (23) and (24) yields

$$\frac{3}{2}\ \rho R T_s + \frac{\rho u^2}{2} = \frac{3}{4}\ \frac{\rho}{\beta^2} = \frac{3}{2}\ \rho R T$$

or

$$T_s = T - \frac{u^2}{3R} \tag{25}$$

For a simple gas, $3R/2 = c_v$ and equation (25) becomes

$$T = T_s + \frac{u^2}{2c_v} \tag{26}$$

The static pressure can readily be obtained from the static temperature by the ideal gas law $p_s = \rho R T_s$.

Total energy leaving surface element. - The total energy per unit area $e_{\lambda_1,t}$ leaving surface λ at point λ_1 is derived in the same manner as equation (27) in reference 2. The accommodation coefficient is defined as

$$\alpha = \frac{e_{\lambda_1,t} - \left(e_{\lambda_1,t}\right)_{in}}{m_{\lambda_1}E_{\lambda_1} - \left(e_{\lambda_1,t}\right)_{in}} \tag{27a}$$

where $\left(e_{\lambda_1,t}\right)_{in}$ is the total energy incident on the surface per unit area and $m_{\lambda_1}E_{\lambda_1}$ is the energy flux that would be carried away from the surface if all the incident molecules achieved thermal equilibrium with the wall. The energy per unit mass of the stream leaving surface λ that is in equilibrium with the wall is shown in equation (A22) to be

$$E_\lambda = \left(c_v + \frac{R}{2}\right)T_\lambda$$

The total energy flux leaving the lower surfaces at point λ_1 is

$$e_{\lambda_1,t} = \alpha m_\lambda E_\lambda + (1 - \alpha)\left[m_L E_L F_{dA_{\lambda_1}-L} + m_R E_R F_{dA_{\lambda_1}-R} + \int_0^l e_{\mu_1,t}K(\lambda_1,\mu_1)d\mu_1\right] \tag{27b}$$

where E_L, the energy per unit mass of the stream entering from the left reservoir, is equal to $[c_v + (R/2)]T_L$, and E_R is defined similarly for the right reservoir. In equation (27b), it is assumed that the accommodation coefficient α is equal for both isothermal walls and all the molecules are leaving the wall diffusely.

When mE_λ, $m_L E_L$, and $e_{\mu_1,t}$ are equal to $e_R = m_R E_R$, equation (27b) shows that $e_{\lambda_1,t} = e_R$. Hence equation (27b) can be written

$$e_{\lambda_1,t} - e_R = \alpha\left(m_{\lambda_1}E_\lambda - e_R\right)$$

$$+ (1 - \alpha)\left[(e_L - e_R)F_{dA_{\lambda_1}-L} + \int_0^l \left(e_{\mu_1,t} - e_R\right)K(\lambda_1,u_1)d\mu_1\right] \tag{28}$$

Similarly, for the upper wall,

$$e_{\mu_1,t} - e_R = \alpha\left(m_{\mu_1}E_\mu - e_R\right)$$

$$+ (1 - \alpha)\left[(e_L - e_R)F_{dA_{\mu_1}-L} + \int_0^l \left(e_{\lambda_1,t} - e_R\right)K(\lambda_1,\mu_1)d\lambda_1\right] \tag{29}$$

Because of the linearity of the problem, the principle of superposition can be used to reduce the problem into simpler parts that can be added together for various boundary conditions as follows:

$$e_{\lambda_1,t} - e_R = \left[\varphi_{1-L}(\lambda_1)\right](e_L - e_R) + \left[\varphi_{1-1A}(\lambda_1)\right]E_\lambda(m_L - m_R)$$

$$+ \left[\varphi_{1-1B}(\lambda_1)\right](m_R E_\lambda - e_R)$$

$$+ \left[\varphi_{1-2A}(\lambda_1)\right]E_\mu(m_L - m_R) + \left[\varphi_{1-2B}(\lambda_1)\right](m_R E_\mu - e_R) \tag{30}$$

$$e_{\mu_1,t} - e_R = \left[\varphi_{1-L}(\mu_1)\right](e_L - e_R) + \left[\varphi_{1-2A}(\mu_1)\right]E_\lambda(m_L - m_R)$$

$$+ \left[\varphi_{1-2B}(\mu_1)\right](m_R E_\lambda - e_R)$$

$$+ \left[\varphi_{1-1A}(\mu_1)\right]E_\mu(m_L - m_R) + \left[\varphi_{1-1B}(\mu_1)\right](m_R E_\mu - e_R) \tag{31}$$

where

$$\varphi_{1-L}(\lambda_1) = (1 - \alpha)\left\{F_{dA_{\lambda_1}-L} + \int_0^l \left[\varphi_{1-L}(\mu_1)\right]K(\lambda_1,\mu_1)d\mu_1\right\}$$

and

$$\varphi_{1-L}(\mu_1) = \varphi_{1-L}(\lambda_1)\Big|_{\lambda\to\mu_1} \tag{32}$$

Then

$$\varphi_{1-1A}(\lambda_1) = \alpha f_{\lambda_1} + (1 - \alpha)\int_0^l \left[\varphi_{1-2A}(\mu_1)\right]K(\lambda_1,\mu_1)d\mu_1 \tag{33a}$$

$$\varphi_{1-2A}(\mu_1) = (1 - \alpha)\int_0^l \left[\varphi_{1-1A}(\lambda_1)\right]K(\lambda_1,\mu_1)d\lambda_1 \tag{33b}$$

$$\left.\begin{aligned}\varphi_{1-1A}(\mu_1) &= \varphi_{1-1A}(\lambda_1)\Big|_{\lambda_1=\mu_1} \\ \text{and} \qquad & \\ \varphi_{1-2A}(\mu_1) &= \varphi_{1-2A}(\lambda_1)\Big|_{\lambda_1=\mu_1}\end{aligned}\right\} \tag{33c}$$

$$\varphi_{1-1B}(\lambda_1) = \alpha + (1 - \alpha)\int_0^{l} \left[\varphi_{1-2B}(\mu_1)\right]K(\lambda_1,\mu_1)d\mu_1 \tag{34a}$$

$$\varphi_{1-2B}(\mu_1) = (1 - \alpha)\int_0^{l} \left[\varphi_{1-1B}(\lambda_1)\right]K(\lambda_1,\mu_1)d\lambda_1 \tag{34b}$$

$$\left.\begin{aligned}\varphi_{1-1B}(\mu_1) &= \varphi_{1-1B}(\lambda_1)\Big|_{\lambda_1\to\mu_1} \\ \text{and} \qquad & \\ \varphi_{1-2B}(\mu_1) &= \varphi_{1-2B}(\lambda_1)\Big|_{\lambda_1\to\mu_1}\end{aligned}\right\} \tag{34c}$$

As shown, the functional dependence of the φ functions on μ_1 is the same as the dependence on λ_1.

These subsolutions possess physical significance. If T_μ and T_L are equal to T_R, while the lower surface is at T_λ, and if $m_L = m_R$, that is, the densities as well as the temperatures of the left and right environments are equal, then the total energy leaving the lower surface is $e_{\lambda_1,t} = e_R + \varphi_{1-1B}(m_R E_\lambda - e_R)$ and the energy leaving the upper surface is $e_{\mu_1,t} = e_R + \varphi_{1-2B}(m_R E_\lambda - e_R)$. The curves for φ_{1-1B} and φ_{1-2B} are given in figure 8 for various values of l. It can readily be seen that the limiting cases for $l = 0$ are $(\varphi_{1-1B})_{l\to 0} = \alpha$ and $(\varphi_{1-2B})_{l\to 0} = 0$, those for $l = \infty$ are $(\varphi_{1-1B})_{l\to\infty} = \frac{1}{2 - \alpha}$ and $(\varphi_{1-2B})_{l\to\infty} = \frac{1 - \alpha}{2 - \alpha}$. The results are symmetrical around $x/l = 0.5$. In the limit as $\alpha \to 0$, the solution reduces to $\varphi_{1-1B} = \varphi_{1-2B} = 0$, while in the limiting case of $\alpha = 1$, the solution reduces to $\varphi_{1-1B} = 1$ and $\varphi_{1-2B} = 0$.

Similarly, if $T_\lambda = T_\mu = T_R$, $m_L = m_R$, and $T_L \neq T_R$, the energy leaving either surface is given by $e_{\lambda_1,t} = e_R + \varphi_{1-L}(e_L - e_R)$. These results are given in figure 9. The limiting solution for $l = 0$ is $(\varphi_{1-L})_{l\to 0} = \frac{1 - \alpha}{2}$, for $l \to \infty$ is $(\varphi_{1-L})_{l\to\infty} = 0$, for $\alpha = 1$ is $\varphi_{1-L} = 0$, and for $\alpha = 0$ is the same

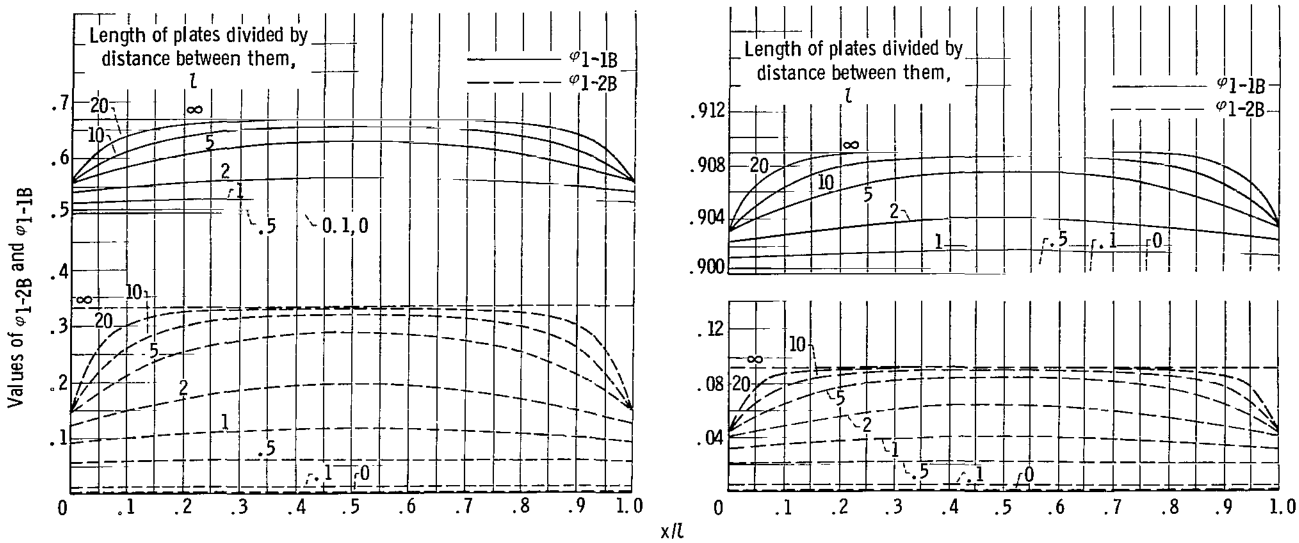

(a) Accommodation coefficient, $\alpha = 0.5$.

(b) Accommodation coefficient, $\alpha = 0.9$.

Figure 8. - Subsolutions $\varphi_{1\text{-}1B} \equiv \left[\frac{e_{x_1,t} - e_R}{m_R(E_1 - E_R)}\right]_{1\text{-}1B}$ and $\varphi_{1\text{-}2B} \equiv \left[\frac{e_{x_2,t} - e_R}{m_R(E_1 - E_R)}\right]_{1\text{-}2B}$.

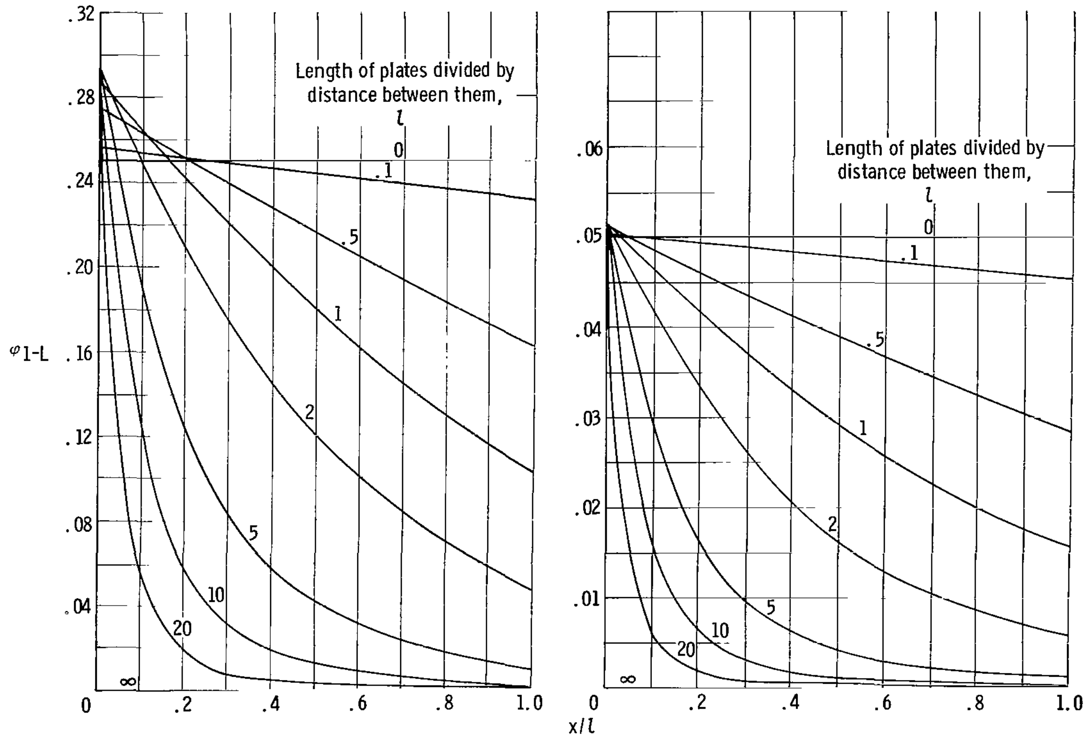

(a) Accommodation coefficient, $\alpha = 0.5$.

(b) Accommodation coefficient, $\alpha = 0.9$.

Figure 9. - Solution $\varphi_{1\text{-}L} \equiv \left(\frac{e_{x_1,t} - e_R}{e_L - e_R}\right)_{1\text{-}L}$.

as equation (3) and is given in figure 2 (p. 6).

Finally, if $T_\lambda = T_\mu = T_R$ and $e_L = e_R$ but $m_L \neq m_R$, then the total energy leaving either surface is given by $e_{\lambda_1,t} = e_R + (m_L - m_R)E_R(\varphi_{1-1A} + \varphi_{1-2A})$. The results for φ_{1-1A} and φ_{1-2A} are shown in figure 10. For $l = 0$, the solution reduces to $\varphi_{1-1A} = \frac{\alpha}{2}$ and $\varphi_{1-2A} = 0$.

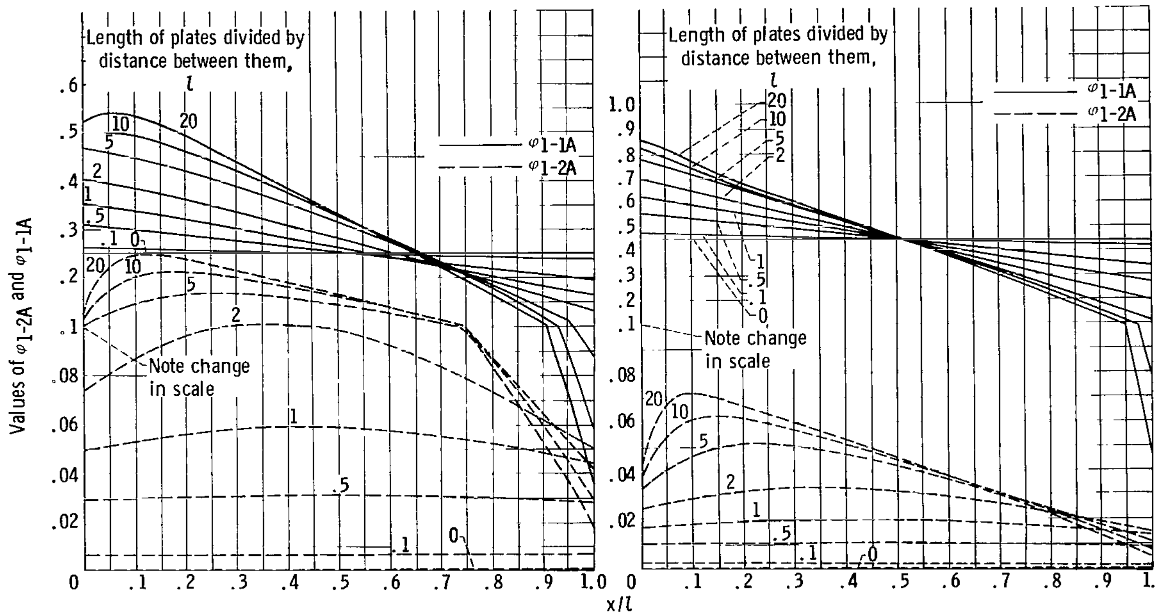

(a) Accommodation coefficient, α = 0.5.

(b) Accommodation coefficient, α = 0.9.

Figure 10. - Subsolutions $\varphi_{1-1A} \equiv \left[\frac{e_{x_1,t} - e_R}{E_1(m_L - m_R)}\right]_{1-1A}$ and $\varphi_{1-2A} \equiv \left[\frac{e_{x_2,t} - e_R}{E_1(m_L - m_R)}\right]_{1-2A}$

Net Energy Leaving Surface

The average net rate at which energy leaves surface λ per unit area of surface is the difference between the rates of emitted and absorbed energy; that is,

$$\frac{Q_\lambda}{A_\lambda} = \frac{\alpha E_\lambda}{l}\int_0^l m_{\lambda_1}\, d\lambda_1 - \frac{\alpha}{l}\int_0^l \left(e_{\lambda_1,t}\right)_{in} d\lambda_1 \tag{35}$$

Substituting

$$e_{\lambda_1,t} = (1 - \alpha)\left(e_{\lambda_1,t}\right)_{in} + \alpha m_{\lambda_1} E_\lambda \tag{36}$$

into equation (35) results in

$$\frac{Q_\lambda}{A_\lambda} = \frac{\alpha}{(1 - \alpha)l} \int_0^l \left(E_\lambda m_\lambda - e_{\lambda_1,t} + e_R - e_R\right) d\lambda_1 \tag{37}$$

Since $\frac{1}{l} \int_0^l f_{\lambda_1}\, d\lambda_1 = \frac{1}{2}$ because $f_{\lambda_1} = 1 - f_{\hat{\lambda}_1}$, equation (37) becomes

$$\frac{Q_\lambda}{A_\lambda} \frac{1 - \alpha}{\alpha} = E_\lambda \frac{m_L - m_R}{2} - e_R - \left(\overline{e_{\lambda_1,t} - e_R}\right) \tag{38}$$

where the bar denotes the integrated average value. Similarly, the average net heat flux leaving wall μ is

$$\frac{Q_\mu}{A_\lambda} = \frac{\alpha}{(1 - \alpha)l} \int_0^l \left(E_\mu m_{\mu_1} - e_{\mu_1,t}\right) d\mu \tag{39}$$

or

$$\frac{Q_\mu}{A_\lambda} \frac{1 - \alpha}{\alpha} = E_\mu \left(\frac{m_L + m_R}{2}\right) - e_R - \left(\overline{e_{\mu_1,t} - e_R}\right) \tag{40}$$

The integrated values $\bar{\varphi} = \frac{1}{l} \int_0^l \varphi\, d\lambda_1$ needed to evaluate $\left(\overline{e_{\lambda_1,t} - e_R}\right)$ and $\left(\overline{e_{\mu_1,t} - e_R}\right)$, which occur in equations (38) and (40), may be evaluated from equations (30) and (31) by using the integrated values $\varphi = \frac{1}{l} \int_0^l \varphi\, d\lambda_1$ given in figure 11.

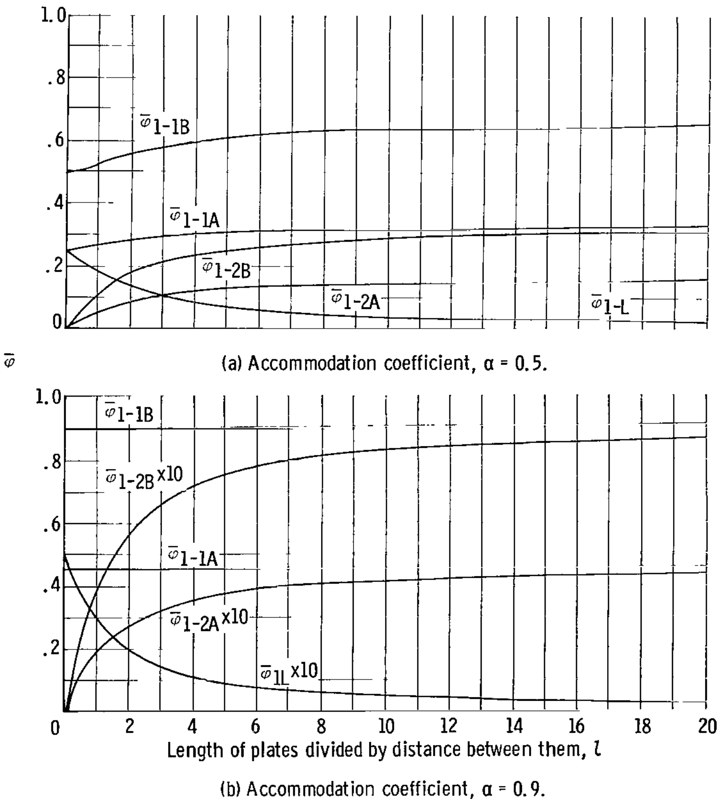

Figure 11. - Integrated mean values of subsolution $\bar{\varphi} = \frac{1}{l} \int_0^l \varphi\, dx$.

Net Energy From Environment

The net energy flux entering the channel through the left end is equal to

$$\frac{Q_L}{A_L} = m_L E_L - \int_0^l e_{\lambda_1,t} F_{dA_{\mu_1}-L}\, d\lambda_1 - \int_0^l e_{\mu_1,t} F_{dA_{\mu_1}-L}\, d\mu_1 - m_R E_R$$

$$\times \left(1 - 2\int_0^l F_{dA_{\lambda_1}-R}\, d\lambda_1\right) \qquad (41)$$

which can be written as

$$\frac{Q_L}{A_L} = m_L E_L - m_R E_R - \int_0^l \left(e_{\lambda_1,t} - e_R\right) F_{dA_{\lambda_1}-L}\, d\lambda_1$$

$$- \int_0^l \left(e_{\mu_1,t} - e_R\right) F_{dA_{\mu_1}-L}\, d\mu_1 \qquad (42)$$

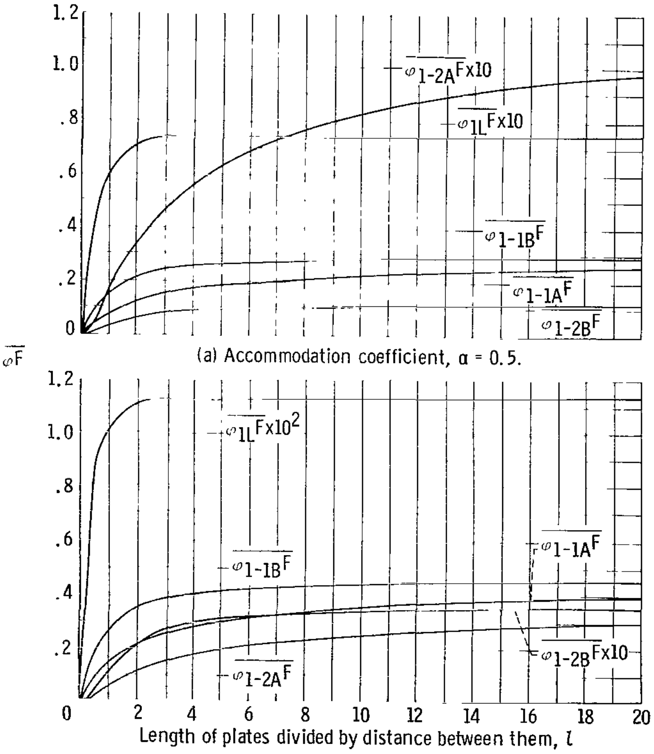

(a) Accommodation coefficient, $\alpha = 0.5$.

(b) Accommodation coefficient, $\alpha = 0.9$.

Figure 12. - Integrated values $\overline{\varphi F} = \int_0^l \varphi F\, dx$.

which is equal to

$$\frac{Q_L}{A_L} = e_L - e_R - \left[\overline{\left(e_{\lambda_1,t} - e_R\right) F_{dA_{\lambda_1}-L}}\right]$$

$$- \left[\overline{\left(e_{\mu_1,t} - e_R\right) F_{dA_{\mu_1}-L}}\right] \qquad (43)$$

Figure 12 shows the integrated results for $\overline{\varphi_{1L}F}$, $\overline{\varphi_{1-1A}F}$, $\overline{\varphi_{1-2A}F}$, $\overline{\varphi_{1-2B}F}$, and $\overline{\varphi_{1-1B}F}$, where $\overline{\varphi F} = \int_0^l \varphi F\, d\lambda_1$. Using these terms with equations (30) and (31) gives Q_L/A_L. By conservation of energy, the net energy flux from the right side is

$$\frac{Q_R}{A_R} = -\frac{Q_L}{A_L} - l\left(\frac{Q_\lambda}{A_\lambda} + \frac{Q_\mu}{A_\mu}\right) \qquad (44)$$

RADIATION HEAT TRANSFER

In most cases where the free-molecule flow is important, the thermal radiation will also be important. The radiation problem involves equations similar to those for the free-molecule flow. The model here is similar to the one treated in reference 6, although the analysis of reference 6 did not include the effects of the right and left environments.

From an energy balance, the total energy leaving point λ_1 by radiation for the present model is

$$e_{\lambda_{1,t}} = \alpha e_\lambda + (1 - \alpha)\left[e_L F_{dA_{\lambda_1}-L} + e_R F_{dA_{\lambda_1}-R} + \int_0^l e_{\mu_{1,t}} K(\lambda_1, u_1) d\mu_1\right] \tag{45}$$

In this case, $e_{\lambda_{1,t}}$ is the total energy leaving point λ_1 by radiation, and e_L and e_R for this case are equal to σT_L^4 and σT_R^4, respectively. The emissivity of the surfaces is given by α. Equation (45) can also be written as

$$e_{\lambda_{1,t}} - e_R = \alpha(e_\lambda - e_R) + (1 - \alpha)\left[(e_L - e_R)F_{dA_{\lambda_1}-L} + \int_0^l \left(e_{\mu_{1,t}} - e_R\right)K(\lambda_1, \mu_1) d\mu_1\right] \tag{46}$$

A similar equation would apply for surface μ

$$e_{\mu_{1,t}} - e_R = \alpha(e_\mu - e_R) + (1 - \alpha)\left[(e_L - e_R)F_{dA_{\mu_1}-L} + \int_0^l \left(e_{\lambda_{1,t}} - e_R\right)K(\lambda_1, \mu_1) d\lambda_1\right] \tag{47}$$

Since this equation is linear, it can be reduced to simpler parts by superposition

$$e_{\lambda_{1,t}} - e_R = \varphi_{1-1B}(\lambda_1)(e_\lambda - e_R) + \varphi_{1-2B}(\lambda_1)(e_\mu - e_R) + \varphi_{1L}(\lambda_1)(e_L - e_R) \tag{48a}$$

and

$$e_{\mu_{1,t}} - e_R = \varphi_{1-2B}(\mu_1)(e_\lambda - e_R) + \varphi_{1-1B}(\mu_1)(e_\mu - e_R) + \varphi_{1L}(\mu_1)(e_L - e_R) \tag{48b}$$

where the φ's are the same relations given in equations (32) and (34).

The net heat radiated from wall λ can be calculated similarly to the free-molecule case to be

$$\frac{Q_\lambda}{A_\lambda} = \frac{\alpha}{(1 - \alpha)l} \int_0^l \left(e_\lambda - e_{\lambda_1,t}\right) d\lambda_1 \tag{49}$$

which becomes

$$\frac{Q_\lambda}{A_\lambda} \frac{1 - \alpha}{\alpha} = e_\lambda - e_R - \left(\overline{e_{\lambda_1,t} - e_R}\right) \tag{50}$$

The term $e_{\lambda_1,t} - e_R$ is obtained by finding the integrated average value of equation (48) by means of figure 11. Similarly, for the upper surface μ,

$$\frac{Q_\mu}{A_\lambda} \frac{1 - \alpha}{\alpha} = e_\mu - e_R - \left(\overline{e_{\mu_1,t} - e_R}\right) \tag{51}$$

The energy entering from the left end is also obtained as before:

$$\frac{Q_L}{A_L} = e_L - e_R - \int_0^l \left(e_{\lambda_1,t} - e_R\right) F_{dA_{\lambda_1}-L}\, d\lambda_1 - \int_0^l \left(e_{\mu_1,t} - e_R\right) F_{dA_{\mu_1}-L}\, d\mu \tag{52}$$

which can be written as

$$\frac{Q_L}{A_L} = e_L - e_R - \overline{\left(e_{\lambda_1,t} - e_R\right) F_{dA_{\lambda_1}-L}} - \overline{\left(e_{\mu_1,t} - e_R\right) F_{dA_{\mu_1}-L}} \tag{53}$$

Equation (44) can be used to find Q_R.

EXAMPLE

For purposes of illustration and to indicate the magnitude of the free-molecule heat transfer, a sample calculation is carried out. Consider the case where the left and right environments and one wall are at equal temperatures and the densities of the left and right environments are equal while the other wall is at temperature T_λ. This type of situation is similar to one that may arise in a thermionic energy converter. For this case, the free-molecule heat transfer from equations (30) and (38) is

$$\left(\frac{Q_\lambda}{A_\lambda}\right)_c = \left[\frac{\alpha m_R (E_\lambda - E_R)}{1 - \alpha}\right]_c \left(1 - \overline{\varphi}_{1-1B}\right) \tag{54}$$

Similarly, for radiation from equations (48) and (50)

$$\left(\frac{Q_\lambda}{A_\lambda}\right)_r = \left[\frac{\alpha(e_\lambda - e_R)}{1 - \alpha}\right]_r (1 - \overline{\varphi}_{1-1B}) \tag{55}$$

Dividing equation (54) by equation (55) yields

$$\frac{Q_{\lambda,c}}{Q_{\lambda,r}} = \left[\frac{1 - \alpha}{\alpha(e_\lambda - e_R)}\right]_r \left[\frac{\alpha m_R(E_\lambda - E_R)}{1 - \alpha}\right]_c \tag{56}$$

The gas is assumed to be argon at a density of 10^{-4} ρ_s, where ρ_s is the density at standard conditions (273° K and 1 atm) and the plates are assumed to be tungsten with plate 1 at 2000° K and plate 2 at 500° K. The wall emissivity is taken equal to 0.3. Hence, the radiation factor on the right side of equation (56) is

$$\left[\frac{1 - \alpha}{\alpha\sigma\left(T_\lambda^4 - T_R^4\right)}\right]_r = 0.107 \frac{(\text{sq cm})(\text{sec})}{\text{cal}}$$

In the evaluation of the convection factor of this equation, the accommodation coefficient for the argon-tungsten combination is given in reference 7 as 0.85. Also,

$$m_R = \rho_R\left(\frac{RT_R}{2\pi}\right)^{1/2} = 2.296\times10^{-3} \frac{\text{g}}{(\text{sq cm})(\text{sec})}$$

Since $c_v = (3/2)R$ for argon, equation (22) is used to obtain

$$E_\lambda - E_R = 2R(T_\lambda - T_R) = 149 \text{ cal/g}$$

Combining these results gives

$$\frac{Q_{\lambda,c}}{Q_{\lambda,r}} = 0.21$$

which indicates that the free-molecule-flow heat transfer is not negligible for conditions that might occur in a thermionic device. This ratio, however, will depend strongly on the conditions chosen. For higher wall temperatures than those chosen here the radiation heat transfer will increase because the radiation depends on the temperature to the fourth power. For higher densities, the free-molecule heat transfer will increase since it is directly proportional to the density. At high densities, however, the present solutions are no longer applicable because the mean free path will be small compared with the channel width, and the effect of intermolecular collisions cannot be neglected.

The dimension of the channel for free-molecule flow to occur can be found if the mean free path of the gas molecule is known. For hard sphere molecules, the mean free path L_m is given by

$$L_m = \frac{1}{\sqrt{2}\,\pi m \sigma_m^2}$$

where σ_m is the molecular diameter. Table 1.6 of reference 7 gives for argon

$$L_m = 6.2\times10^{-6}\,\frac{\rho_s}{\rho}\ \mathrm{cm}$$

For ρ_s/ρ of 10^4, $L_m = 0.062$ centimeter, which is large compared with the distances between the plates commonly used in thermionic energy converters. Therefore, the assumption of this report that the effects of molecular collisions are negligible in thermionic converters appears reasonable.

CONCLUDING REMARKS

The present results give solutions for the density, mass flow, wall shear, static temperature, and pressure distributions in a flat-plate channel with free-molecule flow. Calculations are carried out to indicate values of these flow characteristics for different conditions. Also found is the heat transfer between the surfaces and the environment by free-molecule flow and by thermal radiation for arbitrary combinations of temperatures. A comparison of the radiation heat transfer with the free-molecule heat transfer in a sample case that is similar to that existing in a thermionic converter shows that free-molecule heat transfer can be significant when compared with radiative heat transfer.

Lewis Research Center
National Aeronautics and Space Administration
Cleveland, Ohio, August 24, 1964

APPENDIX - MASS FLUX TRANSFER BETWEEN SURFACE ELEMENTS

The mass flux through an elemental area $dA_{x'}$ at some point x', which is assumed to have a gas in a Maxwellian distribution behind it is given by $m_{x'}$. The mass flow from $dA_{x'}$ that is incident on an elemental area dA_x due to molecules in the speed range V to $V + dV$ can be obtained from reference 1 in the following way (see fig. 1, p. 5):

$$dA_x \, dm_{dA_{x'}-dA_x,dV} = \frac{2m_{x'}\beta_{x'}^4 V^3 \exp\left(-\beta_{x'}^2 V^2\right) dV \cos\psi_{x'} \, dA_{x'}}{s^2\pi} \cos\psi_x \, dA_x \tag{A1}$$

which can be rewritten as

$$dA_x \, dm_{dA_{x'}-dA_x,dV} = m_{x'} 2\beta_{x'}^4 V^3 \exp\left(-\beta_{x'}^2 V^2\right) dV \, dF_{dA_{x'}-dA_x} \, dA_{x'} \tag{A2}$$

The term $dF_{dA_{x'}-dA_x}$ is the same as the shape factors used in thermal radiation. After equation (A2) is integrated over V from 0 to ∞, it becomes

$$\left.\begin{aligned} dA_x \, dm_{dA_{x'}-dA_x} &= m_{x'} \, dF_{dA_{x'}-dA_x} \, dA_{x'} \\ &\text{or} \\ dm_{dA_{x'}-dA_x} &= m_{x'} \, dF_{dA_x-dA_{x'}} \end{aligned}\right\} \tag{A3}$$

where use was made of the following reciprocal relation often used in radiation:

$$dF_{dA_{x'}-dA_x} \, dA_{x'} = dF_{dA_x-dA_{x'}} \, dA_x = \frac{\cos\psi_{x'} \cos\psi_x \, dA_{x'} \, dA_x}{\pi s^2}$$

Since m_{μ_1} is independent of μ_3, the integration over μ_3 can be carried out and the shape factor evaluated for an infinite strip of width $d\mu_1$ on the upper wall at point μ_1 to an elemental area in the lower channel wall dA_{λ_1}. Figure 1 (p. 5) shows that $\cos\psi_{\lambda_1} = \frac{r\cos\theta}{s}$ and $\cos\psi_{\mu_1} \, d\mu_1 \, d\mu_3 = \frac{r^2 \, d\theta \, d\mu_3}{s}$, where $s^2 = r^2 + \mu_3^2$. This gives

$$dF_{dA_{\lambda_1}-d\mu_1} = (\cos\theta \, d\theta) \frac{r^3}{\pi} \int_{-\infty}^{+\infty} \frac{d\mu_3}{s^4} = \frac{d(\sin\theta)}{2} \tag{A4}$$

This result is similar to that found in reference 8.

The total mass flux incident on and therefore reflected from an elemental area dA_{λ_1} is

$$m_{\lambda_1} = \int_{-\pi/2}^{\pi/2} \frac{m_\theta}{2} d(\sin \theta) = \int_{-\infty}^{+\infty} m_{\mu_1} K(\lambda_1,\mu_1) d\mu_1 \tag{A5}$$

where m_θ is the mass flux emitted from a surface element that is oriented at angle θ with respect to the normal to the point λ_1 on the lower plate as shown in figure 1(b). For $\mu_1 < 0$, $m_{\mu_1} = m_L$, while, for $\mu_1 > l$, $m_{\mu_1} = m_R$. Since

$$\sin \theta = \frac{\mu_1 - \lambda_1}{\left[(\mu_1 - \lambda_1)^2 + 1\right]^{1/2}} \tag{A6}$$

then

$$K(\lambda_1,\mu_1) d\mu_1 = \frac{d\mu_1}{2\left[(\mu_1 - \lambda_1)^2 + 1\right]^{3/2}} \tag{A7}$$

The exchange factor from the left reservoir to dA_{λ_1} is given by

$$F_{dA_{\lambda_1}-L} = \int_{-\pi/2}^{\theta_L} \frac{d(\sin \theta)}{2} = \frac{1}{2}\left[1 - \frac{\lambda_1}{\left(\lambda_1^2 + 1\right)^{1/2}}\right] \tag{A8}$$

since in this case $m_{\mu_1} = m_L$, a constant.

Local Density Distribution

If there are $d\rho_{dA_{x'},dV}/M$ molecules per unit volume in front of an elemental area dA_x at some point x that originate at an elemental area $dA_{x'}$ at some point x' having speeds in the range V to $V + dV$, the flux through dA_x at velocity V is as follows (see fig. 1, p. 5):

$$dA_x \, dm_{dA_{x'}-dA_x,dV} = V \cos \psi_x \, dA_x \, d\rho_{dA_{x'},dV} \tag{A9}$$

Setting equation (A1) equal to (A9) gives

$$d\rho_{dA_{x'},dV} = \frac{2\beta_{x'}^4 m_{x'} V^2 \exp\left(-\beta_{x'}^2 V^2\right) dV \cos \psi_{x'} \, dA_{x'}}{\pi s^2} \tag{A10}$$

If the previous expression is integrated over both V and the depth, the density at point x in the channel may be expressed as

$$\rho = \frac{1}{\pi^{1/2}} \int_0^{2\pi} \beta_\theta m_\theta \, d\theta \qquad \text{(A11a)}$$

Notice that the limits on the integral now extend over all angles, inasmuch as a point within the channel (and not on a wall) receives molecules from the two reservoirs and the two walls, and these particles all contribute to ρ. Since $\theta = \tan^{-1}\left[(\mu_1 - x_1)/\hat{x}_2\right]$ for the upper wall,

$$d\theta = \frac{\hat{x}_2 \, d\mu_1}{\hat{x}_2^2 + (\mu_1 - x_1)^2} \qquad \theta_0 \leq \theta \leq \theta_l \qquad \text{(A11b)}$$

A similar result holds true for the lower wall.

Local Longitudinal Flux

As in reference 1, the local mass flux through the channel is obtained by multiplying the density component $d\rho_{d\mu_1 d\mu_3, dV}$ by the component of molecular velocity in the x_1-direction to give

$$d(\rho u_1)_{d\mu_1 d\mu_3, dV} = d\rho_{d\mu_1 d\mu_3, dV} \frac{V(x_1 - \mu_1)}{s}$$

$$= 4\beta_{\mu_1}^4 m_{\mu_1}^3 V^3 \exp\left(-\beta_{\mu_1}^2 V^2\right) dV \cos \psi_{\mu_1} \frac{(x_1 - \mu_1) d\mu_1 \, d\mu_3}{2\pi s^3} \qquad \text{(A12)}$$

Treating this expression as equation (A11a) was treated in the previous section results in

$$\rho u_1 = -\int_0^{2\pi} \frac{m_{\mu_1}}{2} \sin \theta \, d\theta \qquad \text{(A13)}$$

Since $\cos \theta = \hat{x}_2 / \left[(x_1 - \mu_1)^2 + \hat{x}_2^2\right]^{1/2}$, then, for the upper wall,

$$-\frac{\sin \theta}{2} \, d\theta = \frac{\hat{x}_2 (x_1 - \mu_1) d\mu_1}{2\left[(x_1 - \mu_1)^2 + \hat{x}_2^2\right]^{3/2}} \qquad \text{(A14)}$$

Local Transverse Flux

The flux in the x_2 or transverse direction is obtained by multiplying the density component by the component of molecular velocity in the x_2-direction. For the present model

$$d(\rho u_2)_{d\mu_1 d\mu_3,dV} = d\rho_{d\mu_1 d\mu_3,dV}\, V\, \frac{x_2 - 1}{s} \tag{A15}$$

which yields

$$\rho u_2 = -\int_0^{2\pi} \frac{m_\theta}{2} \cos\theta\, d\theta \tag{A16}$$

Since $\sin\theta = \mu_1 - x_1/\left[(\mu_1 - x_1)^2 + \hat{x}_2^2\right]^{1/2}$, then, for the upper wall,

$$\frac{\cos\theta\, d\theta}{2} = \frac{\hat{x}_2^2\, d\mu_1}{2\left[(\mu_1 - x_1)^2 + \hat{x}_2^2\right]^{3/2}} \tag{A17}$$

Shear stress in x_1-direction along wall. - The shear stress in the x_1-direction on the surface λ due to the molecules having speeds in the range V to $V + dV$ coming from the direction θ from the elemental area $d\mu_1\, d\mu_3$ is

$$-d(\rho\overline{V_1V_2})_{w_{d\mu_1 d\mu_3,dV}} = d\rho_{d\mu_3 d\mu_1,dV}\, \frac{V^2}{s^2}\, (\lambda_1 - \mu_1) \tag{A18}$$

This can be integrated to obtain

$$d(\rho\overline{V_1V_2})_{w_{d\mu_1}} = \frac{m_\theta}{\beta_\theta \pi^{1/2}} \cos\theta \sin\theta\, d\theta \tag{A19}$$

Energy transfer between wall elements. - The energy of each molecule in the stream from $dA_{x'}$ to dA_x (assuming a Maxwellian distribution behind $dA_{x'}$ corresponding to a temperature equal to $T_{x'} = 1/2R\beta_{x'}^2$, can be written as equal to $(1/2)MV^2 + MU_{x'}$ where $MU_{x'}$ is the average nontranslational internal energy of the molecule at temperature $T_{x'}$. Combining the energy of each molecule with equation (A2) results in

$$\int_V dA_x\, dm_{dA_{x'}-dA_x,dV}\left(\frac{1}{2} V^2 + U_{x'}\right) = \left(U_{x'} + \frac{1}{\beta_{x'}^2}\right) m_{x'}\, dF_{dA_x - dA_{x'}}\, dA_x \tag{A20}$$

Since $U_{x'} = \left[c_v - (3/2)R\right]T_{x'}$, equation (A20) becomes

$$m_{x'}E_{x'}\, dF_{dA_x - dA_{x'}}\, dA_x = m_{x'}\left(c_v + \frac{R}{2}\right)T_{x'}\, dF_{dA_x - dA_{x'}}\, dA_x \tag{A21}$$

where $E_{x'}$, the total energy per unit mass of the molecular stream at x', satisfies the relation

$$E_{x'} = \left(c_v + \frac{R}{2}\right)T_{x'} \tag{A22}$$

REFERENCES

1. Kennard, E. H.: Kinetic Theory of Gases. McGraw-Hill Book Co., Inc., 1938.

2. Sparrow, E. M., Jonsson, V. K., and Lundgren, T. S.: Free-Molecule Tube Flow and Adiabatic Wall Temperatures. Jour. Heat Transfer (Trans. ASME), ser. C, vol. 85, no. 2, May 1963, pp. 111-118.

3. Sparrow, E. M., and Jonsson, V. K.: Free-Molecule Flow and Convective-Radiative Energy Transport in a Tapered Tube or Conical Nozzle. AIAA Jour., vol. 1, no. 5, May 1963, pp. 1081-1087.

4. Chahine, M. T.: Free Molecule Flow Over Nonconvex Surfaces. Proc. Int. Symposium on Rarefied Gas Dynamics, L. Talbot, ed., Academic Press, Inc., 1961.

5. Clausing, P.: The Flowing of Very Dilute Gases Through Tubes of any Length. Ann. Phys., vol. 12, no. 8, Mar. 1932, pp. 961-989.

6. Sparrow, E. M.: Application of Variational Methods to Radiation Heat-Transfer Calculations. Jour. Heat Transfer (Trans. ASME), ser. C, vol. 82, no. 4, Nov. 1960, pp. 375-380.

7. Dushman, Saul: Scientific Foundations of Vacuum Technique. John Wiley & Sons, Inc., 1962.

8. Jakob, M.: Heat Transfer. Vol. 2. John Wiley & Sons, Inc., 1957, p. 21.

2-17185 -6

"The aeronautical and space activities of the United States shall be conducted so as to contribute . . . to the expansion of human knowledge of phenomena in the atmosphere and space. The Administration shall provide for the widest practicable and appropriate dissemination of information concerning its activities and the results thereof."

—NATIONAL AERONAUTICS AND SPACE ACT OF 1958

NASA SCIENTIFIC AND TECHNICAL PUBLICATIONS

TECHNICAL REPORTS: Scientific and technical information considered important, complete, and a lasting contribution to existing knowledge.

TECHNICAL NOTES: Information less broad in scope but nevertheless of importance as a contribution to existing knowledge.

TECHNICAL MEMORANDUMS: Information receiving limited distribution because of preliminary data, security classification, or other reasons.

CONTRACTOR REPORTS: Technical information generated in connection with a NASA contract or grant and released under NASA auspices.

TECHNICAL TRANSLATIONS: Information published in a foreign language considered to merit NASA distribution in English.

TECHNICAL REPRINTS: Information derived from NASA activities and initially published in the form of journal articles.

SPECIAL PUBLICATIONS: Information derived from or of value to NASA activities but not necessarily reporting the results of individual NASA-programmed scientific efforts. Publications include conference proceedings, monographs, data compilations, handbooks, sourcebooks, and special bibliographies.

Details on the availability of these publications may be obtained from:

SCIENTIFIC AND TECHNICAL INFORMATION DIVISION

NATIONAL AERONAUTICS AND SPACE ADMINISTRATION

Washington, D.C. 20546